International Journal of Thermophysics, Vol. 26, No. 4, July 2005 (© 2005)
DOI: 10.1007/s10765-005-6725-5

IR Radiative Properties of Solid and Liquid Alumina: Effects of Temperature and Gaseous Environment[1]

V. Sarou-Kanian,[2,3] J. C. Rifflet,[2] and F. Millot[2]

An infrared spectrometer (spectral range 2–6 μm), coupled with a 9 μm pyrometer (Christiansen's wavelength), has been developed to collect time-resolved measurements (32 spectra/s) of the spectral emissivity of alumina droplets ($d \approx 3$ mm) freely cooling in an aerodynamic levitation system from the liquid-to-solid phases [2800 → 1500 K]. The temperature and nature of the gaseous atmosphere surrounding the droplet (oxidizing/neutral/reducing) are two important parameters affecting the spectral emissivity in the semi-transparent range. Observations are discussed in the framework of the thermal activation and of the chemical interactions of alumina with the environment.

KEY WORDS: emissivity; extinction coefficient; high temperature; liquid alumina; radiative properties; solid alumina.

1. INTRODUCTION

The radiative properties of solid and liquid alumina at high temperature have been studied during the last 40 years [1–6]. All of these studies have been performed on self-contained liquid alumina, some of them on levitated droplets and some others with the liquid in contact with solid alumina. Most of the published works concern the visible region (0.63 μm), and take also into account the different behaviors under argon and oxygen as well as other gases. A review was published by two of the authors [7], and the influence of the nature and the pressure of the gas in contact with liquid alumina were recognized as significant parameters.

[1] Paper presented at the Seventh International Workshop on Subsecond Thermophysics, October 6–8, 2004, Orléans, France.

[2] CRMHT/CNRS, 1D avenue de la Recherche Scientifique, 45071 Orléans Cedex 2, France.
[3] To whom correspondence should be addressed. E-mail: sarou@cnrs-orleans.fr

Contrary to the visible part of the spectrum, it was also reported [3] that the emissivity of millimeter-sized drops at 10.6 μm is higher than 0.9. Only one study is concerned with the 1–100 μm wavelength range [8] near the melting temperature, using an alumina plate heated in air with a CO_2 laser. On the other hand, various studies on liquid alumina clouds ejected from solid rocket motors have been reported, and have been reviewed by Parry and Brewster [9]. They indicate that the extinction coefficient of liquid alumina in the 1–5 μm spectral range shows a minimum in the middle of this domain.

In the present study, we have developed a dispersive spectrometer to determine the radiative properties from 2 to 6 μm wavelength of 3 mm sized alumina droplets in the temperature range 1500–2800 K and under various atmospheres (oxidizing/inert/reducing). The results are discussed and compared with literature data.

2. EXPERIMENTAL

The experimental set-up is shown in Fig. 1.

2.1. Heating and Levitation

The aerodynamic levitation device consists mainly of a metallic convergent/divergent nozzle (aluminum alloy) with 60° angles and a 2 mm nozzle throat diameter. The sample is completely trapped inside the nozzle,

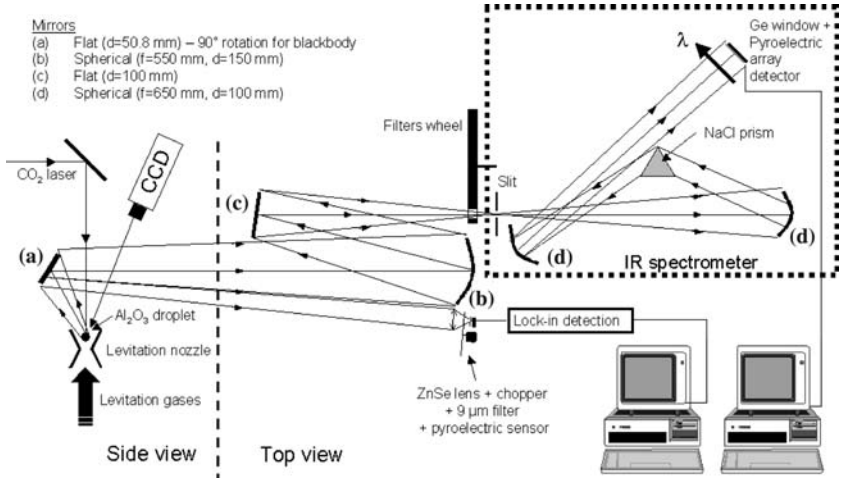

Fig. 1. Experimental set-up.

and an appropriate adjustment of the gas flow ($1–21 \cdot \text{min}^{-1}$) allows a very stable levitation for 50 mg (≈ 3 mm diameter) alumina droplets.

Heating of the droplet is performed with a 30–800 W CO_2 laser working at $\lambda = 10.6\,\mu\text{m}$ (Coherent Everlase 525). With a beam diameter of 13 mm, part of the beam is directly absorbed by the sample (top hemisphere), and another part is first reflected on the walls of the nozzle and is then sent to the sample (top and bottom hemispheres). A 100 W laser power is sufficient to melt the droplet in a few seconds, and it can be maintained in the liquid phase up to 3000 K for hours.

2.2. Temperature Measurements

The droplet surface temperature is measured with an optical pyrometer working at $\lambda = 9\,\mu\text{m}$ which collects part of the light emitted by the droplet and reflected by the flat mirror (a—coated aluminum, $d = 50.8$ mm). The pyrometer includes a zinc selenide (ZnSe) lens ($d = 50.8$ mm, $f = 125$ mm), a bandpass filter (8.5–9.5 μm) centered at 9 μm, a pyroelectric detector, an optical chopper ($f = 86$ Hz), and a lock-in amplifier. The output signal is transferred via a 12-bit PCI-card control and recorded with a computer (data acquisition frequency $f = 500$ Hz). The wavelength was carefully chosen because it is close to the Christiansen's wavelength of alumina [8] that corresponds to a spectral emissivity of 0.999 independent of both the temperature and the nature of the environment. The bandpass filter of the pyrometer was also chosen to avoid any radiation coming from the laser ($\lambda = 10.6\,\mu\text{m}$). The droplet temperature is directly extracted from Planck's law expressed as

$$\frac{U}{U_{\text{cal}}} = \frac{\varepsilon_\lambda^T}{\varepsilon_\lambda^{T_{\text{cal}}}} \frac{e^{\frac{C_2}{\lambda T_{\text{cal}}}} - 1}{e^{\frac{C_2}{\lambda T}} - 1} \tag{1}$$

where U is the output voltage obtained from the pyroelectric detector, ε_λ^T is the spectral emissivity of the material at wavelength λ and at temperature T, C_2 is the second radiation constant ($= 14,388\,\mu\text{m} \cdot \text{K}$, [10]) and subscript "cal" corresponds to the calibration data. Because $\varepsilon_{9\mu m}^T$ is constant for all T at $\lambda = 9\,\mu\text{m}$, Eq. (1) becomes

$$T = \frac{C_2}{\lambda \ln\left(1 + \frac{U_{\text{cal}}}{U}\left(e^{\frac{C_2}{\lambda T_{\text{cal}}}} - 1\right)\right)} \tag{2}$$

Figure 2 illustrates a typical example of the evolution of the surface temperature of alumina droplet free cooling under O_2. At the recalescence,

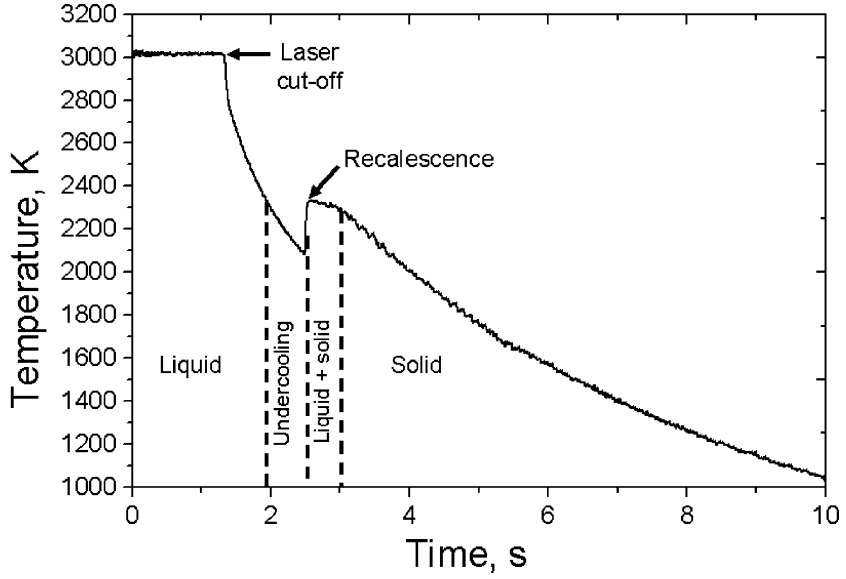

Fig. 2. Temperature of an alumina droplet cooling freely under O_2.

the droplet is characterized by a liquid–solid mixture with a homogeneous temperature corresponding to the melting temperature of alumina ($T_{cal} = 2327 \pm 6$ K [11]). The output voltage at the recalescence (U_{cal}) is used to calibrate the pyrometer.

2.3. Spectrometer

The infrared spectrometer was specifically developed for this study. The major part of the light reflected on the first flat mirror (a) is collected with a first spherical mirror (b—coated aluminum, $d = 150$ mm, $f = 550$ mm) and focused on the entrance slit of the spectrometer via a second flat mirror (c—coated aluminum, $d = 100$ mm). The optical magnification is equal to unity, and the solid angle is 1.46×10^{-2} sr.

The spectrometer is a classical dispersive one. The light from the entrance slit (variable width <1.6 mm) is collected by a second spherical mirror (d—coated aluminum, $d = 100$ mm, $f = 650$ mm) and is sent as parallel light to a sodium chloride equilateral prism (monocrystal NaCl, side length 70 mm, height 60 mm) working at the minimum deviation angle. NaCl was chosen because it transmits the light in a large IR range (0.8–12 μm) with small dispersion (compared to a CaF_2 prism, for example). The split wavelengths are then collected by a third spherical mirror

(d—same characteristics as the second one) and are finally focused on a pyroelectric array detector consisting of 128 elements (DIAS Infrared System, Germany) and protected by a germanium window. The spectra acquisition frequency is 32 Hz and each spectrum is 15-bit digitalized and synchronized with the temperature measurement.

The wavelength calibration is performed with a set of calibrated band-pass filters covering the range 1–10 μm (Northumbria Optical Coatings Ltd.) placed on a filter wheel in front of the entrance slit. In the present work, we have studied the mid-IR spectral range 2–6 μm. The theoretical wavelength resolution varies from 25 to 50 nm, but depends practically on both the entrance slit width (convolution process) and the detection system (modulation transfer function), and is estimated to be between 0.1 and 0.3 μm.

The energy calibration is obtained with a blackbody furnace made of an alumina cavity heated inside a graphite furnace. The temperature of the blackbody cavity is measured with a Pt/(Pt–10% Rh) thermocouple. In order to keep the same optical path for the droplet and the blackbody reference, the first flat mirror is only rotated at 90° in the horizontal plane in front of the blackbody. Various temperatures are then scanned (1200–1900 K) for the calculation and validation of the apparatus function expressed as

$$f_\lambda = \frac{I_\lambda}{L^{\circ}_\lambda(T_{\mathrm{bb}})} = I_\lambda \frac{\lambda^5}{C_1}\left(e^{\frac{C_2}{\lambda T_{\mathrm{bb}}}} - 1\right) \tag{3}$$

where f_λ and I_λ are, respectively, the apparatus function and the intensity count of the pyroelectric element at the wavelength λ, $L^{\circ}_\lambda(T_{\mathrm{bb}})$ is the spectral luminance of the blackbody at temperature T_{bb}, and C_1 is the first radiation constant ($=3.741 \times 10^{-16}\,\mathrm{W \cdot m^2}$, [10]). Figure 3a,b illustrates, respectively, the evolution of the intensity counts of the pyroelectric detector and the apparatus function Vs. the wavelength for six temperatures. We can observe that f_λ varies weakly with T ($\Delta f_\lambda / f_\lambda < 3\%$) showing that the energy response of the spectrometer is linear for all the wavelengths.

3. RESULTS

The experimental procedure is always the same. First, the droplet is heated with the laser and kept at a fixed temperature for about 1 min. The laser is then switched off, and spectra and temperature measurements are recorded and processed only during the free cooling. Indeed, under the laser beam, the top hemisphere of the droplet is overheated leading to an important gradient of temperature (up to 200 K between top and bottom).

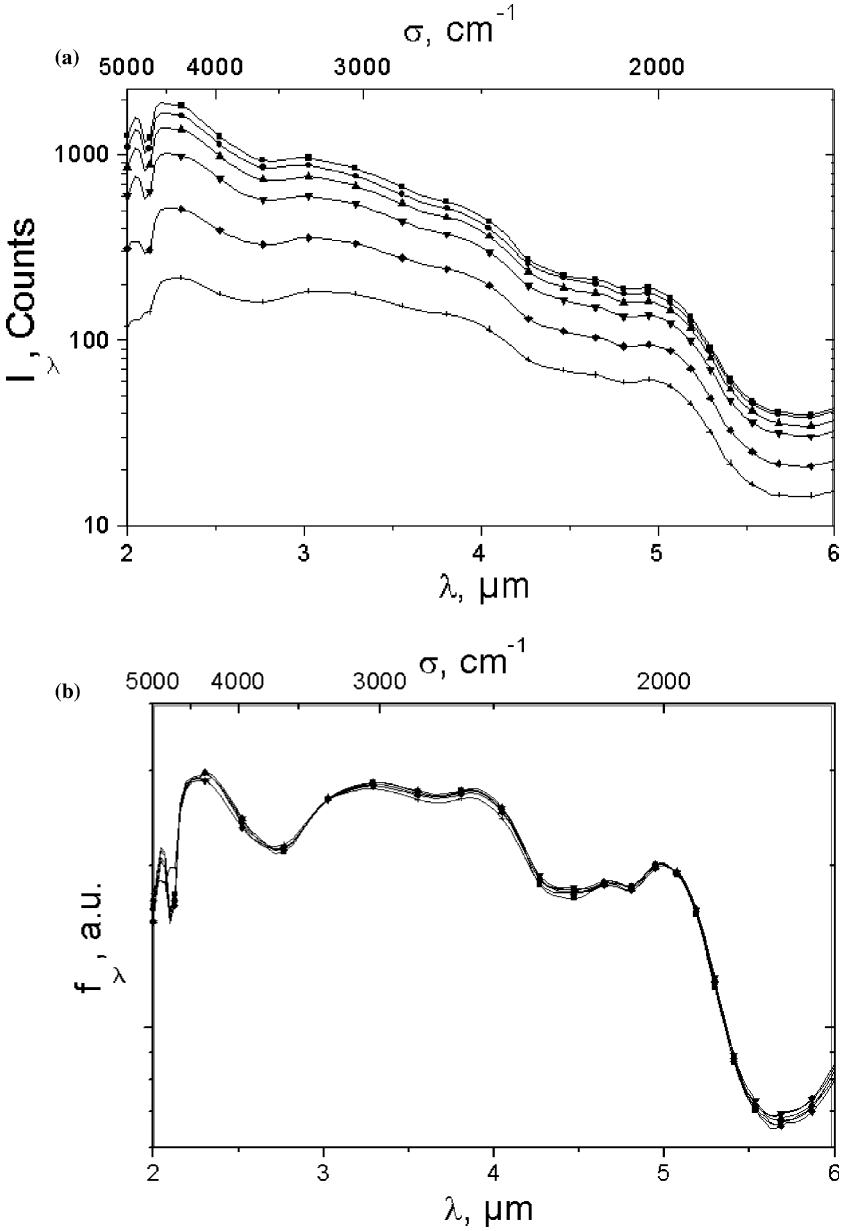

Fig. 3. Intensity counts of the pyroelectric detector (a) and apparatus function of the spectrometer (b) for six blackbody temperatures. (■)$T = 1173$ K; (●)$T = 1393$ K; (▲)$T = 1633$ K; (▼)$T = 1663$ K; (♦)$T = 1753$ K; +, $T = 1923$ K.

On the contrary, when the laser stops, the temperature rapidly tends to be homogeneous in the droplet after 100 ms [11]. In the liquid state, the temperature homogenization is promoted by convection inside the droplet. In the solid state, the temperature gradient between the surface and the core of the sphere is higher than in the liquid state (no more internal convection); by only considering the thermal conduction (Fourier's law) for heat transfer inside the sphere, the maximum temperature gradient core-surface is estimated within a few 10° at 2300 K.

The spectral emissivity is theoretically defined as

$$\varepsilon_\lambda^T = \frac{L_\lambda(T)}{L_\lambda^o(T)} \tag{4}$$

where $L_\lambda(T)$ is the spectral luminance at temperature T of the material. Practically, ε_λ^T is deduced from the expression:

$$\varepsilon_\lambda^T = \frac{I_\lambda}{f_\lambda}\frac{\lambda^5}{C_1}\left(e^{\frac{C_2}{\lambda T}} - 1\right) \tag{5}$$

The following results representing the spectral emissivity in the 2–6 μm range as a function of the temperature for solid and liquid alumina have been obtained on droplets levitating in O_2, Ar, or Ar + 5%H_2.

Figures 4a, b and 5a, b illustrate the evolution of the spectral emissivity in the 2–6 μm range of liquid and solid alumina for different temperatures in O_2 and Ar. Note that the results in Ar + 5%H_2 are similar to those in Ar.

In the liquid phase, it is observed that alumina is opaque in O_2 for $T > 2500$ K, and then becomes more and more transparent in the 2–4.8 μm when the temperature decreases to the undercooled liquid with a minimum located between 3 and 3.5 μm (Fig. 4a, $\varepsilon_{\min} \approx 0.3$) in agreement with Ref. 9. However, alumina in Ar or Ar/5% H_2 (Fig. 5a) is always opaque for all temperatures, and is characterized by small or an absence of undercooling.

In the solid phase, it is observed that the emissivity of alumina in O_2 (Fig. 4b) decreases in two stages, rapidly between the first point of recalescence ($T_{\text{recal.}} = 2327$ K), and $T = 2200$ K, then slowly below this last temperature. In Ar or Ar/5% H_2 (Fig. 5b), the emissivity also decreases but slower than in O_2. For example, $\varepsilon_{3\,\mu m}(O_2, T = 1500\,\text{K}) \approx 0.03$ is about 16 times less than $\varepsilon_{3\,\mu\text{m}}(\text{Ar or Ar/H}_2, T = 1500\,K) \approx 0.5$.

Figure 6 shows the evolution of the spectral emissivity at $\lambda = 3\,\mu$m for liquid and solid alumina in the temperature range (1500–2800 K) and for O_2 and Ar atmospheres. The main differences which were pointed out previously between the two atmospheres (the semi-transparency of liquid alumina in O_2 below $T = 2500$ K contrary to the unvarying opacity in Ar,

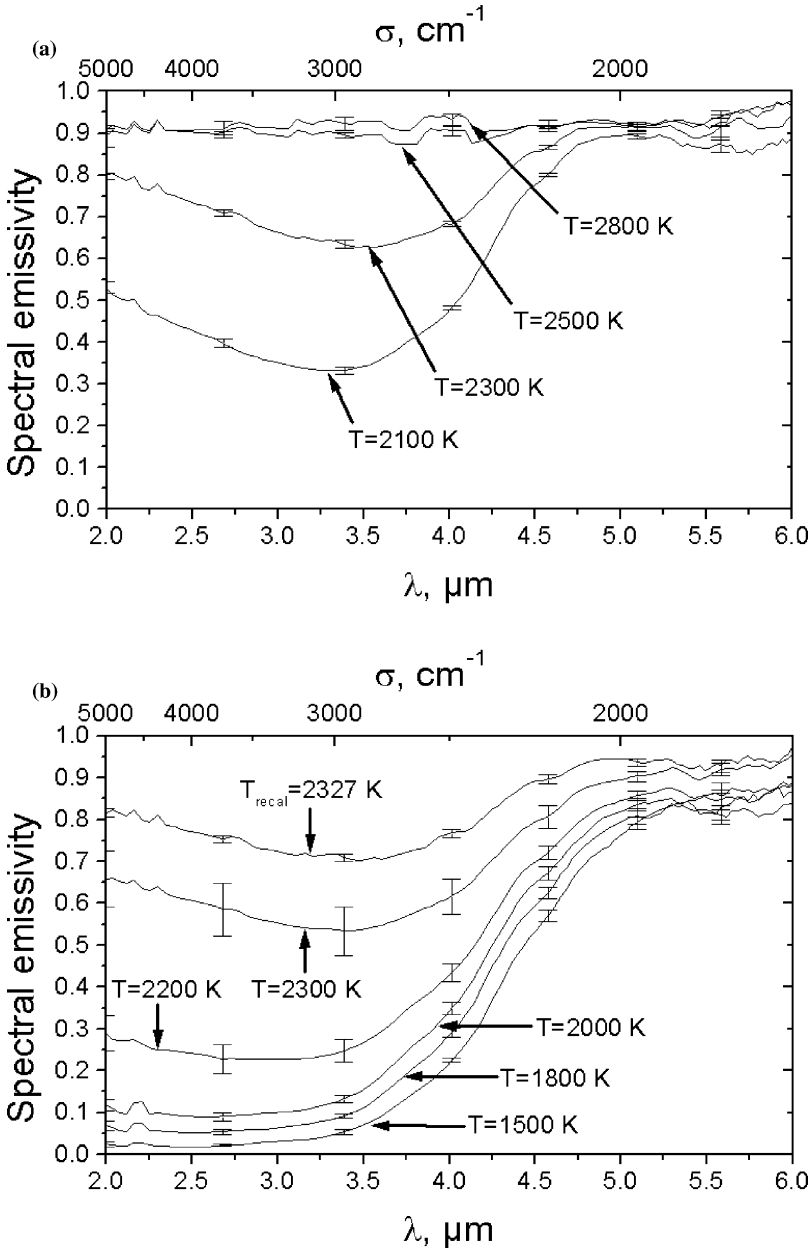

Fig. 4. Spectral emissivity of alumina in O_2 vs. temperature: (a) liquid; (b) liquid + solid and solid.

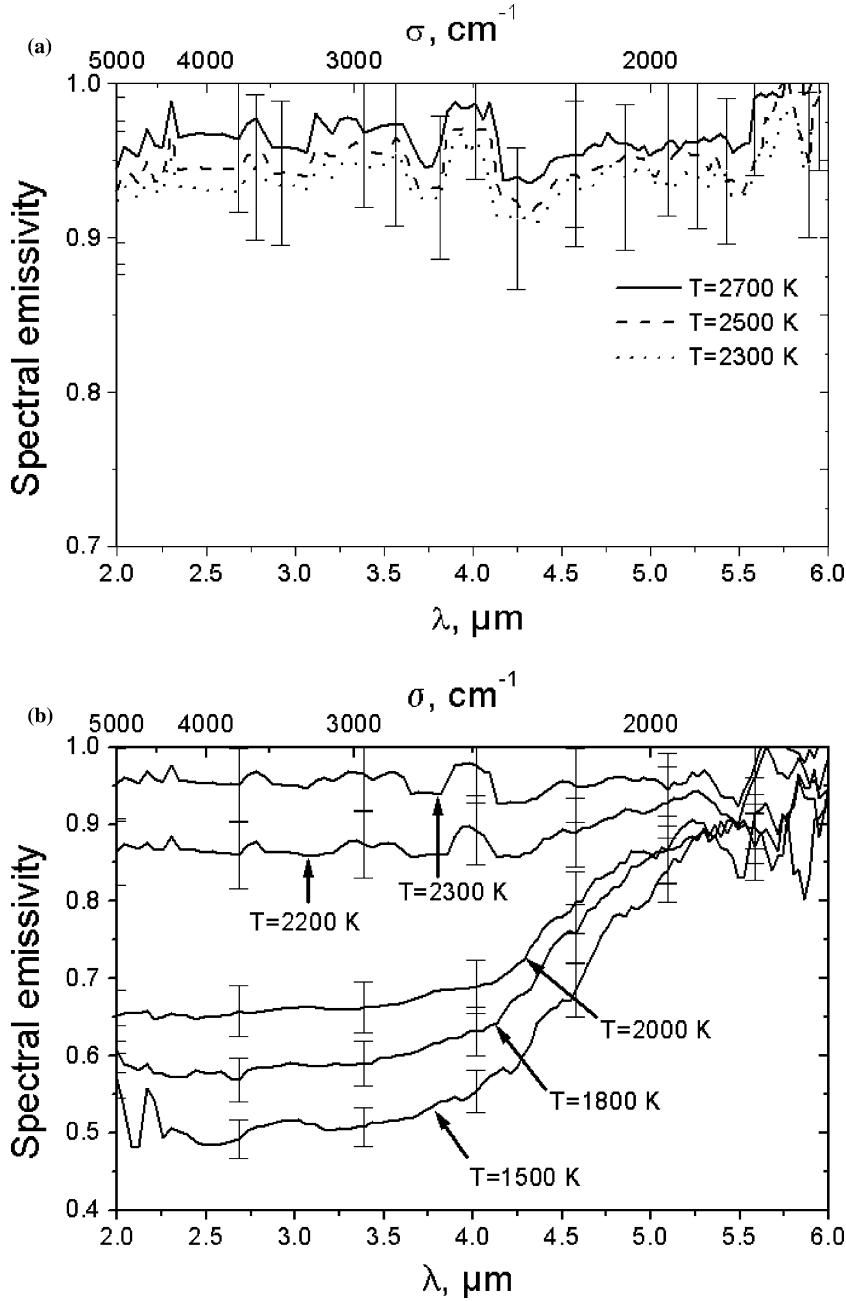

Fig. 5. Spectral emissivity of alumina in Ar vs. temperature: (a) liquid; (b) liquid + solid and solid.

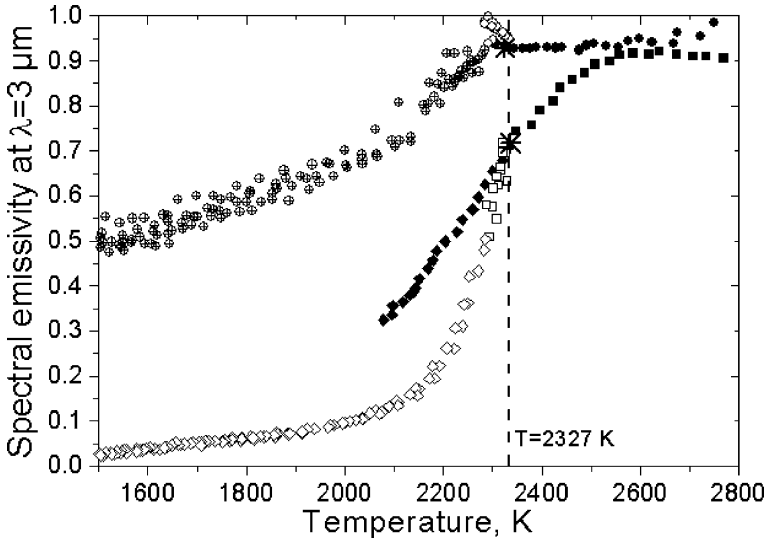

Fig. 6. Spectral emissivity of solid and liquid alumina in O_2 and Ar at 3 μm vs. temperature. In O_2: (■) liquid, (♦) undercooled liquid, (□) liquid + solid, (◊) solid; in Ar: (●) liquid, (○) liquid + solid, (⊕) solid; (∗) first point of recalescence.

solid alumina is more emissive in Ar than in O_2) are clearly shown. One can also notice that the undercooled liquid in O_2 is more emissive than the solid at the same temperature. The same emissivity is obtained for the liquid at $T = 2327$ K and for the liquid + solid state at the first instant of the recalescence phenomenon. After the recalescence, the emissivity slightly increases nearly up to unity in Ar, while it rapidly decreases in O_2.

4. DISCUSSION

The main observation concerning the present results is that the emissivities of solid and liquid alumina droplets depend strongly on the temperature and on the nature of the gaseous environment in the semi-transparent range from 2 to 5 μm.

The temperature effect is particularly significant near the melting point of alumina. This phenomenon was already observed previously [2, 3, 8, 9]. This fact suggests that the emissivity of alumina both in liquid and solid states is thermally activated. Figure 7 illustrates the evolution of the extinction coefficient at 3 μm (k_λ) as a function of temperature by considering an Arrhenius law dependence ($\ln(k_\lambda) = f(1/T)$). k_λ is deduced from

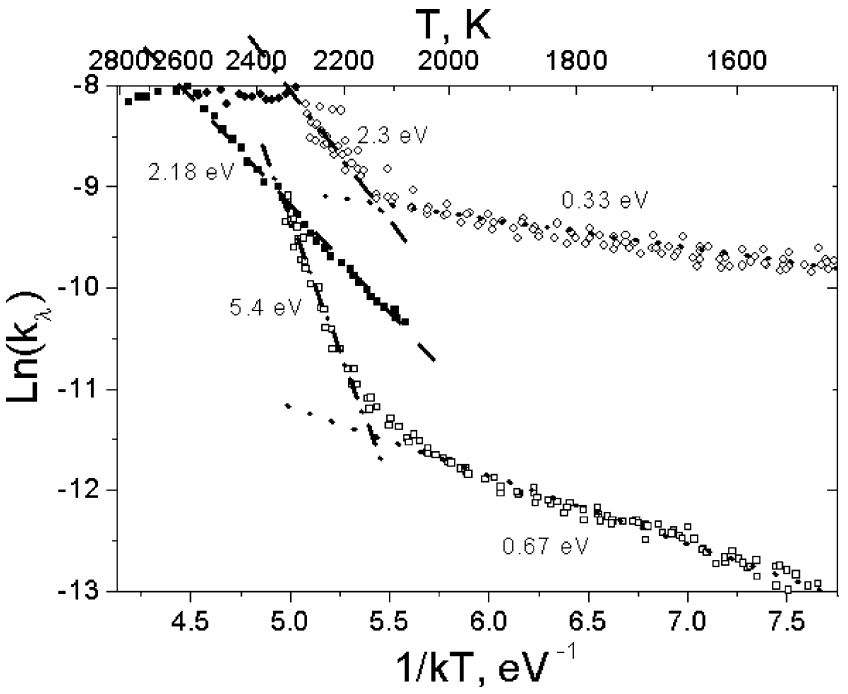

Fig. 7. Extinction coefficient of solid and liquid alumina in O_2 and Ar at 3 μm vs. temperature. In O_2: (■) liquid, (□) liquid + solid/solid; in Ar: (●) liquid, (○) liquid + solid/solid.

the emissivity of a semi-transparent medium of thickness d expressed as

$$\varepsilon_\lambda = (1 - R_\lambda)\,\frac{1 - \exp\left(\frac{4\pi k_\lambda d}{\lambda}\right)}{1 - R_\lambda \exp\left(\frac{4\pi k_\lambda d}{\lambda}\right)} \tag{6}$$

where R_λ is the spectral reflectivity estimated as $R_\lambda = 0.07$ at 3 μm [7]. Apart from the opacity range (k_λ is constant), two or three linear regimes can be easily identified corresponding to the nature of alumina: the liquid and undercooled liquid (only in O_2), the solid in the temperature range (1500–2200 K), and the intermediate zone near fusion (2200–2327 K). The estimation of the activation energies (E_a in eV, slope of the linear regression) confirms that the temperature effect (in O_2) is higher in the liquid ($E_a = 2.18$ eV) than in the solid (0.67 eV), and that it is even stronger near the fusion for all atmospheres (5.4 eV in O_2 and 2.3 eV in Ar, respectively, 8 and 7 times higher than in the solid state). The presence of this

intermediate zone is quite questionable, but it is considered to correspond to a particular state of alumina when the solidification process and the first step of cooling occur. Indeed, after the recalescence and during the solidification, the alumina droplet consists of a liquid–solid mixture with a thick solid layer growing from the surface which may have completely different optical properties than pure solid and liquid phases. Previous authors [2, 8] studying the temperature effect on the optical properties of alumina in the opposite thermal path (solid $\rightarrow$ liquid) have generally observed a sudden gap at the phase change. This difference between the discontinuity of the optical properties in the solid/liquid transition and the continuity in the liquid/solid transition were also considered by Anfimov et al. [12].

The effect of the gaseous environment on the emissivity of alumina in the semi-transparent range with obvious differences between oxidizing and neutral/reducing atmospheres was also observed by Refs. 1, 3, 4, and 5. In fact, this influence of the nature of gases on the radiative properties can be explained by the thermal history of liquid alumina at high temperature and the consequences on its composition. Indeed, in O_2 at $T = 3200\,K$, liquid alumina seems to be quite stable; no evaporation process is observed (no decrease of the droplet size). However, in Ar or Ar/5% H_2 at the same temperature, there is a significant evaporation process; alumina is decomposed in gaseous aluminum oxides (Al_2O, AlO,...) which condense again in the gas flow forming visible smoke above the aerodynamic levitation system. Furthermore, after cooling, the observation of the samples at ambient temperature shows that they are white in O_2, but grey in Ar or Ar/H_2 (in the visible). Coutures et al. [11] already noticed this phenomenon, and they found that there were small clusters of metallic aluminum inside the grey samples. This fact suggests that liquid alumina, heated up to 3200 K and evaporating in inert/reducing gases, is non-stoichiometric alumina with a lack of oxygen (Al_2O_{3-x}). Thus, when the droplet cools freely after this thermal treatment, it has probably not enough time to become stoichiometric, and it maintains this non-stoichiometry in both the liquid and solid phases. Weber et al. [3] have shown that alumina contaminated with small amounts of metals (Fe, Mg, Si, W) was opaque at $\lambda = 0.663\,\mu m$ and $T = 2400\,K$. In a way, it can be considered that the excess of aluminum in the droplet acts as a contaminant of alumina and involves in its opacity.

Furthermore, it should be reminded that liquid alumina in O_2 also cannot be considered as stoichiometric: there are no reasons that alumina does not contain an excess of oxygen (Al_2O_{3+x}) in this case. The optical properties of alumina in O_2 may therefore not characterize the stoichiometric compound, i.e., lower spectral emissivities in the 2–5 μm range. This hypothesis is an interesting issue for future work.

5. CONCLUSION

The present work describes the development of an infrared spectrometer and the first results obtained from the measurements of spectral emissivities in the (2–6 μm) range for solid and liquid alumina droplets at high temperature (1500–2800 K). The effects of temperature and gaseous atmospheres were particularly investigated. It was shown that the spectral emissivity strongly depends upon both parameters. Alumina is more emissive in inert/reducing gases than in O_2. Liquid alumina is always opaque in Ar or Ar/5%H_2 whereas it becomes transparent below $T \approx 2500$ K in O_2 with a minimum located at 3–3.5 μm. The temperature effect exists in all atmospheres, but is stronger in O_2, and is particularly high near the fusion (2200–2327 K). These observations demonstrate that the spectral emissivity is thermally activated with different regimes according to the nature of the phase (solid, liquid, or solid+liquid), and depends on the composition of alumina (non-stoichiometry).

REFERENCES

1. J. K. R. Weber, S. Krishnan, C. D. Anderson, and P. C. Nordine, *J. Am. Ceram. Soc.* **78:** 583 (1995).
2. M. Bober, H. U. Karow, and K. Muller, *High Temp. High Press.* **12:** 161 (1980).
3. J. K. R. Weber, P. C. Nordine, and S. Krishnan, *J. Am. Ceram. Soc.* **78:** 3067 (1995).
4. L. S. Nelson, N. L. Richardson, K. Keil, and S. R. Skaggs, *High Temp. Sci.* **5:** 138 (1973).
5. J. J. Diamond and A. L. Dragoo, *Rev. Hautes Temp. Refract.* **3:** 273 (1966).
6. S. Krishnan, J. K. R. Weber, R. A. Schiffman, and P. C. Nordine, *J. Am. Ceram. Soc.* **74:** 881 (1991).
7. F. Millot, B. Glorieux, and J. C. Rifflet, *AIAA Prog. Astronaut. Aeronaut.* **185:** 777 (2000).
8. O. Rozenbaum, D. De Sousa Meneses, S. Chermanne, Y. Auger, and P. Echegut, *Rev. Sci. Instrum.* **70:** 4020 (1999).
9. D. L. Parry and M. Q. Brewster, *J. Thermophys. Heat Trans.* **5:** 142 (1991).
10. NIST CODATA (2002), website: http://physics.nist.gov/cuu/Constants/index.html
11. J. P. Coutures, J. C. Rifflet, P. Florian, and D. Massiot, *Rev. Int. Hautes Temp. Réfract.* **29:** 123 (1994).
12. N. A. Anfimov, G. F. Karabadjak, B. A. Khmelinin, Y. A. Plastinin, and A. V. Rodionov, *Presented at 28th Thermophysics Conference* (AIAA, Orlando, Florida, 1993).